Article

Catalase#Peroxidase Activity of Iron(III)#TAML Activators of Hydrogen Peroxide

Anindya Ghosh, Douglas A. Mitchell, Arani Chanda, Alexander D. Ryabov, Delia Laura Popescu, Erin C. Upham, Gregory J. Collins, and Terrence J. Collins

J. Am. Chem. Soc., **2008**, 130 (45), 15116-15126 • DOI: 10.1021/ja8043689 • Publication Date (Web): 17 October 2008

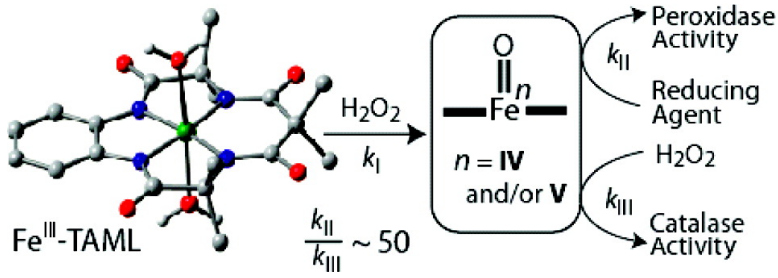

More About This Article

Additional resources and features associated with this article are available within the HTML version:

- Supporting Information
- Access to high resolution figures
- Links to articles and content related to this article
- Copyright permission to reproduce figures and/or text from this article

View the Full Text HTML

J|A|C|S
ARTICLES

Published on Web 10/17/2008

Catalase−Peroxidase Activity of Iron(III)−TAML Activators of Hydrogen Peroxide

Anindya Ghosh, Douglas A. Mitchell, Arani Chanda, Alexander D. Ryabov,*
Delia Laura Popescu, Erin C. Upham, Gregory J. Collins, and Terrence J. Collins*

Department of Chemistry, Carnegie Mellon University, 4400 Fifth Avenue, Pittsburgh, Pennsylvania 15213

Received June 9, 2008; E-mail: tc1u@andrew.cmu.edu

Abstract: Exceptionally high peroxidase-like and catalase-like activities of iron(III)−TAML activators of H_2O_2 (**1:** Tetra-Amidato-Macrocyclic-Ligand Fe^{III} complexes [Fe{1,2−$X_2C_6H_2$−4,5−$(NCOCMe_2NCO)_2CR_2$}(OH_2)]$^-$) are reported from pH 6−12.4 and 25−45 °C. Oxidation of the cyclometalated 2-phenylpyridine organometallic complex, $[Ru^{II}(o\text{-}C_6H_4py)(phen)_2]PF_6$ (**2**) or "ruthenium dye", occurs via the equation $[Ru^{II}] + 1/2\ H_2O_2 + H^+ \xrightarrow{Fe^{III}-TAML} [Ru^{III}] + H_2O$, following a simple rate law $rate = k_{obs}^{per}[\mathbf{1}][H_2O_2]$, that is, the rate is independent of the concentration of **2** at all pHs and temperatures studied. The kinetics of the catalase-like activity ($H_2O_2 \xrightarrow{Fe^{III}-TAML} H_2O + 1/2\ O_2$) obeys a similar rate law: $rate = k_{obs}^{cat}[\mathbf{1}][H_2O_2]$). The rate constants, k_{obs}^{per} and k_{obs}^{cat}, are strongly and similarly pH dependent, with a maximum around pH 10. Both bell-shaped pH profiles are quantitatively accounted for in terms of a common mechanism based on the known speciation of **1** and H_2O_2 in this pH range. Complexes **1** exist as axial diaqua species $[FeL(H_2O)_2]^-$ ($\mathbf{1}_{aqua}$) which are deprotonated to afford $[FeL(OH)(H_2O)]^{2-}$ ($\mathbf{1}_{OH}$) at pH 9−10. The pathways $\mathbf{1}_{aqua} + H_2O_2$ (k_1), $\mathbf{1}_{OH} + H_2O_2$ (k_2), and $\mathbf{1}_{OH} + HO_2^-$ (k_4) afford one or more oxidized Fe−TAML species that further rapidly oxidize the dye (peroxidase-like activity) or a second H_2O_2 molecule (catalase-like activity). This mechanism is supported by the observations that (i) the catalase-like activity of **1** is controllably retarded by addition of reducing agents into solution and (ii) second order kinetics in H_2O_2 has been observed when the rate of O_2 evolution was monitored in the presence of added reducing agents. The performances of the **1** complexes in catalyzing H_2O_2 oxidations are shown to compare favorably with the peroxidases further establishing Fe^{III}−TAML activators as miniaturized enzyme replicas with the potential to greatly expand the technological utility of hydrogen peroxide.

Introduction

Compared with reduction or carbon−carbon bond forming chemistry, oxidation chemistry is relatively devoid of broadly useful homogeneous catalysts. Yet nature practices catalytic oxidation chemistry on a vast scale, leaving chemists with the obvious challenge of learning how to match the enzymes with comparably performing synthetic analogues. Nowhere perhaps is this challenge more alluring than in hydrogen peroxide chemistry where enzymes with exceptional performance have challenged chemists for many decades to match or better them. Millions of tons of hydrogen peroxide are produced annually for use in stoichiometric processes[1] that could be improved by high-performance, low-cost catalysts. In the pursuit of synthetic analogues, much has been learned from landmark studies of the diversity of enzyme reactivity. There are two major classes of peroxide-activating enzymes, the peroxidases and the catalases, both of which are primarily heme-based.[2] Peroxidases transfer two oxidation equivalents from H_2O_2 to reducing substrates,[2,3] whereas catalases promote the disproportionation of H_2O_2 into dioxygen and water.[4−7] The two reactivity channels are often in competition in the chemistry of a single enzyme. Thus, the catalase−peroxidase enzymes perform both functions.[8−14] The catalase-like activity of catalase−peroxidases (ca.

(1) Hage, R.; Lienke, A. *Angew. Chem., Int. Ed.* **2006**, *45*, 206–222.
(2) Dunford, H. B. *Heme Peroxidases*; Wiley-VCH: New York, 1999.
(3) Everse, J.; Everse, K. E.; Grisham, M. B. *Peroxidases in Chemistry and Biology*; CRC Press: Boca Raton, FL, 1991; Vols. I and II.
(4) Zamocky, M.; Koller, F. *Prog. Biophys. Mol. Biol.* **1999**, *72*, 19–66.
(5) Mate, M. J.; Murshudov, G.; Bravo, J.; Melik-Adamyan, W.; Loewen, P. C.; Fita, I. In *Handbook of Metalloproteins*; John Wiley & Sons Ltd.: Chichester, 2001; Vol. 1, pp 486−502.
(6) Nicholls, P.; Fita, I.; Loewen, P. C. *Adv. Inorg. Chem.* **2001**, *51*, 51–106.
(7) Heinze, M.; Gerhardt, B. *Plant Peroxisomes* **2002**, 103–140.
(8) Jakopitsch, C.; Regelsberger, G.; Furtmueller, P. G.; Rueker, F.; Peschek, G. A.; Obinger, C. *Biochem. Biophys. Res. Commun.* **2001**, *287*, 682–687.
(9) Jakopitsch, C.; Regelsberger, G.; Furtmuller, P. G.; Ruker, F.; Peschek, G. A.; Obinger, C. *J. Inorg. Biochem.* **2002**, *91*, 78–86.
(10) Jakopitsch, C.; Auer, M.; Regelsberger, G.; Jantschko, W.; Furtmueller, P. G.; Rueker, F.; Obinger, C. *Biochemistry* **2003**, *42*, 5292–5300.
(11) Jakopitsch, C.; Auer, M.; Regelsberger, G.; Jantschko, W.; Furtmuller, P. G.; Ruker, F.; Obinger, C. *Eur. J. Biochem.* **2003**, *270*, 1006–1013.
(12) Zamocky, M.; Regelsberger, G.; Jakopitsch, C.; Obinger, C. *FEBS Lett.* **2001**, *492*, 177–182.
(13) Powers, L.; Hillar, A.; Loewen, P. C. *Biochim. Biophys. Acta* **2001**, *1546*, 44–54.
(14) Voegtle, H.; Dawson, J. H. *Chemtracts* **2001**, *14*, 12–17.

10.1021/ja8043689 CCC: $40.75

10^6 M^{-1} s^{-1} expressed as the ratio of the catalytic rate constant over the Michaelis constant, i.e., k_{cat}/K_M)[15] is usually higher than their peroxidase-like activity.[10] Certain peroxidases exhibit no substantial catalase activity, for example, cytochrome *c* peroxidase and plant ascorbate peroxidase.[16] Horseradish peroxidase isoenzyme C displays catalase-like activity when H_2O_2 is the only substrate present; the activity is low ($k_{cat}/K_M \approx 10^2-10^3$ M^{-1} s^{-1}).[15,17] In determining how successful any design process for a given synthetic analogue might be, it is obviously important to parametrize the relative peroxidase and catalase activities. The peroxidase activity is almost invariably the valuable reactivity channel, and the catalase activity can be regarded as an unwelcome intruder that wastes peroxide that would otherwise be directed to productive peroxidase-like substrate conversions.

Iron coordination complex mimics with macrocyclic and related ligands of heme-containing catalases and peroxidases are numerous,[18−21] but high performance peroxidase mimics have been elusive until recently. Early catalase models involved colloidal platinum, whereas peroxidases were mimicked largely by iron complex−H_2O_2 systems[22] which usually launch Fenton chemistry.[23] Since the early days,[24] the concepts and principles of creating enzyme mimics have advanced considerably. For synthetic peroxidase mimics, the ligand systems must reproduce a suitable strongly donating electronic structure for enabling access to high valent iron−oxo complexes, but not so donating as to quench the oxidizing properties. This ligand donor capacity feature is one element in a "design domain" that is comprised of a "master strategy" enabled by "design elements" that have been introduced to compensate for the selectivity controlling features lost by discarding the protein in small molecule mimics of the oxidizing enzymes.[25] The most challenging design element to achieve requires a synthetic catalyst's ligand system to resist the fierce oxidizing conditions associated with the targeted oxo complexes for long enough to be functionally useful. This synthetic design element is made less essential to the enzymes by the protein which can channel the reactivity away from enzyme destruction by requiring as in P450 enzymes that the targeted substrate must be present adjacent to the active site before the catalytic cycle is initiated. This ligand robustness synthetic design element and others have been fleshed out through the Fe^{III}−TAML design program.[26] Another important measure of success in peroxidase mimicking research requires a synthetic catalyst to capture the high activity of the enzymes with competition from catalase-like activity being minimal. This is especially important for green chemical mimics because high activity and high peroxidase-like selectivity translates to high atom and energy efficiencies as well as satisfying overarching economic constraints.[27]

Chart 1. Fe^{III}−TAML Activators of Hydrogen Peroxide (**1**) Used in This Study

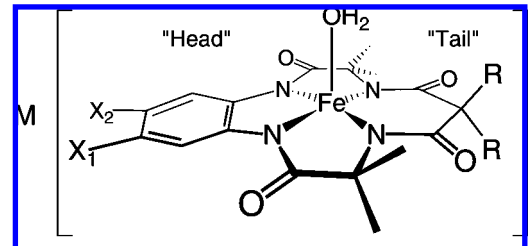

1

	X_1	X_2	R
a	H	H	CH_3
b	NO_2	H	CH_3
c	H	H	F
d	Cl	Cl	F
	MeOOC	H	CH_3
	Cl	Cl	CH_3
	CH_3	H	CH_3
	CH_3	CH_3	CH_3
	COOH	H	CH_3

We have introduced Fe^{III}−TAML activators, a family of low molecular weight green catalysts for the H_2O_2 oxidation of a wide spectrum of targets[26,28,29] including toxic polychlorophenols,[30] thiophosphate pesticides and nitrophenols,[31] azo dyes,[32] dibenzothiophenes,[33] an anthrax surrogate,[34] and natural and synthetic estrogens.[35] These iron catalysts contain a central ferric iron coordinated to the cavity of a tetraanionic tetra-amido-macrocyclic-ligand (TAML), Chart 1. Fe^{III}−TAML activators of H_2O_2 display peroxidase-like activities and longevities[36] that are remarkable for low molecular weight synthetic catalysts. As we show here, in the absence of other reducing agents, Fe^{III}−TAML activators also catalytically convert H_2O_2 into

(15) Hiner, A. N. P.; Hernandez-Ruiz, J.; Williams, G. A.; Arnao, M. B.; Garcia-Canovas, F.; Acosta, M. *Arch. Biochem. Biophys.* **2001**, *392*, 295–302.
(16) Hiner, A. N.; Rodriguez-Lopez, J. N.; Arnao, M. B.; Lloyd Raven, E.; Garcia-Canovas, F.; Acosta, M. *Biochem. J.* **2000**, *348*, 321–328.
(17) Hernandez-Ruiz, J.; Arnao, M. B.; Hiner, A. N. P.; Garcia-Canovas, F.; Acosta, M. *Biochem. J.* **2001**, *354*, 107–114.
(18) Sigel, H. *Angew. Chem., Int. Ed. Engl.* **1969**, *8*, 167–177.
(19) Meunier, B. *Biomimetic Oxidations Catalyzed by Transition Metal Complexes*; Imperial College Press: London, 2000.
(20) Meunier, B. *Models of heme peroxidases and catalases*; Imperial College Press: London, 2000.
(21) Marques, H. M. *Dalton Trans.* **2007**, 4371–4385.
(22) Weiss, J. *J. Phys. Chem.* **1937**, *41*, 1107–1116.
(23) Walling, C. *Acc. Chem. Res.* **1975**, *8*, 125–131.
(24) Bredig, G.; Müller von Berneck, R. Z. *Psysik. Chem.* **1899**, *31*, 258–353.
(25) Collins, T. J.; Gordon-Wylie, S. W.; Bartos, M. J.; Horwitz, C. P.; Woomer, C. G.; Williams, S. A.; Patterson, R. E.; Vuocolo, L. D.; Paterno, S. A.; Strazisar, S. A.; Peraino, D. K.; Dudash, C. A. *In Green Chemistry*; Anastas, P. T., Williamson, T. C., Eds.; Oxford University Press: Oxford, 1998; pp 46−71.
(26) Collins, T. J.; Walter, C. *Sci. Am.* **2006**, *294*, 83–88, 90.
(27) Collins, T. *Science* **2001**, *291*, 48–49.
(28) Collins, T. J. *Acc. Chem. Res.* **1994**, *27*, 279–285.
(29) Collins, T. J. *Acc. Chem. Res.* **2002**, *35*, 782–790.
(30) Sen Gupta, S.; Stadler, M.; Noser, C. A.; Ghosh, A.; Steinhoff, B.; Lenoir, D.; Horwitz, C. P.; Schramm, K.-W.; Collins, T. J. *Science* **2002**, *296*, 326–328.
(31) Chanda, A.; Khetan, S. K.; Banerjee, D.; Ghosh, A.; Collins, T. J. *J. Am. Chem. Soc.* **2006**, *128*, 12058–12059.
(32) Chahbane, N.; Popescu, D.-L.; Mitchell, D. A.; Chanda, A.; Lenoir, D.; Ryabov, A. D.; Schramm, K.-W.; Collins, T. J. *Green Chem.* **2007**, *9*, 49–57.
(33) Mondal, S.; Hangun-Balkir, Y.; Alexandrova, L.; Link, D.; Howard, B.; Zandhuis, P.; Cugini, A.; Horwitz, C. P.; Collins, T. J. *Catal. Today* **2006**, *116*, 554–561.
(34) Banerjee, D.; Markley, A. L.; Yano, T.; Ghosh, A.; Berget, P. B.; Minkley, E. G., Jr.; Khetan, S. K.; Collins, T. J. *Angew. Chem., Int. Ed.* **2006**, *45*, 3974–3977.
(35) Shappell, N. W.; Vrabel, M. A.; Madsen, P. J.; Harrington, G.; Billey, L. O.; Hakk, H.; Larsen, G. L.; Beach, E. S.; Horwitz, C. P.; Ro, K.; Hunt, P. G.; Collins, T. J. *Environ. Sci. Technol.* **2008**, *42*, 1296–1300.
(36) Horwitz, C. P.; Fooksman, D. R.; Vuocolo, L. D.; Gordon-Wylie, S. W.; Cox, N. J.; Collins, T. J. *J. Am. Chem. Soc.* **1998**, *120*, 4867–4868.

Table 1. Equilibrium and Rate Constants (in M^{-1} s^{-1}) and Activation Parameters for the Fe^{III}−TAML-Catalyzed Oxidation of **2** (eq 1) by Hydrogen Peroxide (0.01 M Phosphate)

Fe^{III}−TAML	temperature or activation parameter	$10^{-2} \times k_1$	$10^{-4} \times k_2$	$10^{-6} \times k_3$	$10^{-3} \times k_4$	pK_{a1}	pK_{a2}
1a	25 °C	1.3 ± 1.0	1.2 ± 0.5	0.4 ± 0.2	[a]	9.7 ± 1.0	10.8 ± 2.0
1c	25 °C	4.0 ± 1.8	1.8 ± 0.7	0.8 ± 0.1	1.5 ± 1.0	9.5 ± 0.4	10.9 ± 0.4
	32 °C	8.5 ± 11.6	3.3 ± 0.2	1.3 ± 0.1	4.0 ± 2.4	9.3 ± 0.1	10.4 ± 0.1
	38 °C	9.0 ± 8.8	3.5 ± 0.2	1.2 ± 0.1	3.8 ± 1.7	9.6 ± 0.7	10.4 ± 0.1
	45 °C	12.5 ± 0.7	3.6 ± 0.1	1.8 ± 0.1	5.1 ± 2.3	9.2 ± 0.1	10.9 ± 0.1
	$\Delta H^{\ddagger}$ kJmol^{-1}	42 ± 17	4 ± 4	24 ± 4	38 ± 30		
	$\Delta S^{\ddagger}$ J mol^{-1}K^{-1}	−54 ± 17	−145 ± 12	−49 ± 14	−55 ± 95		

[a] Could not be reliably estimated.

dioxygen. Thus, Fe^{III}−TAML activators are reactive, low molecular weight, functioning analogues of catalase−peroxidase enzymes.[37]

In this contribution, we report on a thorough kinetic and mechanistic evaluation of the catalase and peroxidase activities of the **1** catalysts. The study was developed around the following objectives. First, we wanted to understand the major kinetic features of catalysis by Fe^{III}−TAML activators. Second, the absolute reactivity of the Fe^{III}−TAML activators needed to be estimated for comparison with the relevant catalase and peroxidase enzymes as a measure of the effectiveness of our catalyst design protocol.[26,28,29] Third, by revealing the intimate mechanisms of the catalase and peroxidase activity of the Fe^{III}−TAML activators, we hoped to gain new insight into the mechanisms of catalysis by catalase−peroxidase enzymes. These goals are discussed below in an integrated manner.

Experimental

Materials and Methods. Synthetic procedures for the preparation of the Fe^{III}−TAML activators (**1**) can be found in the recent patents from the Institute for Green Science.[38] The cyclometalated ruthenium(II) complex, $[Ru^{II}(o\text{-}C_6H_4py)(phen)_2]PF_6$ (**2**), was prepared as described elsewhere.[39] Pinacyanol chloride and Orange II dyes were Aldrich reagents. Safranine-O (>95% purity) was used as received. Orange II was purified by passage through a C18-silica gel column with water as eluent. Hydrogen peroxide was purchased from Fluka. All other reagents, components of the buffer solutions, and solvents were at least ACS reagent grade (Aldrich, Aldrich Sure-Seal, Fisher, Acros) and were used as received or purified in an appropriate manner.[40] Spectrophotometric measurements were performed using Hewlett-Packard Diode Array spectrophotometers (models 8452A and 8453) equipped with thermostatted cell holders and automatic 8-cell positioners. Quartz cells (0.1, 1.0, and 10.0 cm) were used for investigation of the spectral properties of **1c** in buffered aqueous solutions to cover the 1.84×10^{-6}−2.30×10^{-3} M concentration range for **1c**.

Spectral and Kinetic Studies of Peroxidase-Like Activity. The stoichiometry of the **1c**-catalyzed oxidation of **2** by H_2O_2 was determined at pH 8.5 and 25 °C in the presence of 3.12×10^{-4} M of complex **2** and 2.5×10^{-5} M of **1c**. Aliquots of H_2O_2 (2.19×10^{-5} M) were added to the solution, which was stirred with a magnetic bar in a 1 cm quartz cell until the dye was completely bleached. After each addition of H_2O_2, the absorbance was allowed to reach a plateau. The molar amount of Ru^{II} oxidized was plotted against the molar amount of H_2O_2 added and the slope of this linear plot indicated the reaction stoichiometry.

Kinetic measurements were performed at pH 6−11.5 in 0.01 M phosphate buffer using doubly distilled water. Complex **2** (5.3 mg) was first dissolved in 1.0 mL of acetonitrile (HPLC grade) and the solution was then transferred into the phosphate buffer (pH 7.0) to afford the Ru^{II} stock solution of 1.87×10^{-3} M. Stock solutions of H_2O_2 were prepared daily from 30% H_2O_2 and standardized by measuring the absorbance at 230 nm ($\varepsilon = 72.8$ M^{-1} cm^{-1}).[41] Other organic peroxides were used as received. Stock solutions of Fe^{III}−TAML activators (1.44×10^{-4} M) were prepared daily in pH 7.0 buffer (0.01 M phosphate). Under such conditions, the demetalation of **1** via the general acid mechanism is negligible.[42] The kinetics of oxidation of Ru^{II} into Ru^{III} was monitored by following an absorbance decrease at 480 nm using the pH independent extinction coefficient of 5.28×10^3 M^{-1} cm^{-1}. The following concentrations of **1**, **2**, and H_2O_2 were used for collecting kinetic data: $(0.32-4.8) \times 10^{-7}$ M, $(0.258-1.96) \times 10^{-4}$ M, and $(0.825-11.1) \times 10^{-4}$ M, respectively. The temperature was varied in the range from 25−45 °C. A typical kinetic run was performed as follows. Phosphate buffer (3 mL) was added to a quartz cuvette with a stopper. Appropriate amounts of stock solutions of **1** and **2** were then added. The reaction was initiated by the addition of an aliquot of the stock solution of H_2O_2. The initial rates were calculated from the absorbance versus time plots using the extinction coefficient for **2** reported above. All initial rates reported are the mean values of at least three determinations. Calculations of the rate constants were carried out using a Sigma Plot 2001 package (Version 7.0). Activation parameters in Table 1 were calculated applying errors in k as weights using an Origin 6.1 package.

Kinetic Studies of Catalase-Like Activity. The stoichiometry and kinetics of dioxygen evolution were monitored with a Clark oxygen electrode with a mylar surface (YSI Yellow springs). The reaction chamber was a 1.5 mL water-jacketed vessel with a magnetic stir bar (Gibson). The electrode was calibrated for absolute O_2 concentrations by injecting 4 μL of a 1 mg mL^{-1} solution of bovine liver catalase (2,350 units per 1 mg, Sigma) to the solution of H_2O_2 (1.5 mL, $\sim 1.8 \times 10^{-3}$ M) at pH 7 (0.1 M phosphate) and monitoring the amount of dioxygen evolved.[43] Stock solutions of H_2O_2 ($\sim$1 M) were prepared daily and standardized as described above. Stock solutions of **1** [$(4-9) \times 10^{-4}$ M] were prepared using HPLC grade water. The solution temperature was kept constant in the range 25−45 °C by circulating water. Typically, an aliquot of the H_2O_2 stock solution was first added to 1.5 mL of the phosphate buffer. The final concentration of H_2O_2 was in the range $(0.01-1.0) \times 10^{-2}$ M. Aliquots of the Fe^{III}−TAML stock solution were added such that the catalyst concentration was in the range $(0.01-1.0) \times 10^{-5}$ M. When the decomposition of H_2O_2 was monitored in the presence of Safranine O or Orange II, an aliquot of a dye stock solution was added [final concentration $(0.01 - 1.0) \times 10^{-3}$ M]

(37) Smulevich, G.; Jakopitsch, C.; Droghetti, E.; Obinger, C. *J. Inorg. Biochem.* **2006**, *100*, 568–585.
(38) Patents: http://www.chem.cmu.edu/groups/Collins/awardpatpub/patents/index.html.
(39) Ryabov, A. D.; Sukharev, V. S.; Alexandrova, L.; Le Lagadec, R.; Pfeffer, M. *Inorg. Chem.* **2001**, *40*, 6529–6532.
(40) Perrin, D. D.; Armarego, W. L. F. *Purification of Laboratory Chemicals*, 3rd ed.; Pergamon Press: Oxford, 1988.
(41) George, P. *Biochem. J.* **1953**, *54*, 267–276.
(42) Polshin, V.; Popescu, D.-L.; Fischer, A.; Chanda, A.; Horner, D. C.; Beach, E. S.; Henry, J.; Qian, Y.-L.; Horwitz, C. P.; Lente, G.; Fabian, I.; Münck, E.; Bominaar, E. L.; Ryabov, A. D.; Collins, T. J. *J. Am. Chem. Soc.* **2008**, *130*, 4497–4506.
(43) Krishna, M. C.; Samuni, A.; Taira, J.; Goldstein, S.; Mitchell, J. B.; Russo, A. *J. Biol. Chem.* **1996**, *271*, 26018–26025.

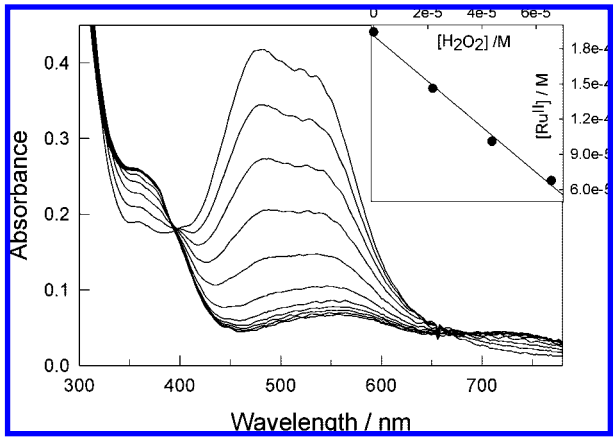

Figure 1. Spectral changes that accompany the catalytic oxidation of **2** by H_2O_2 in the presence **1c**: [**1c**] 1.28×10^{-7} M, [**2**] 5.8×10^{-5} M, [H_2O_2] 3.3×10^{-4} M, pH 9.0 (phosphate buffer 0.01 M), spectra recorded with 5 s intervals. (Inset) Decrease in absorbance on successive additions of aliquots of H_2O_2 at [**1c**] 1.28×10^{-7} M, [**2**] 3.12×10^{-4} M, [H_2O_2] 2.19×10^{-5} M per aliquot, pH 8.5.

prior to the catalyst addition. The kinetic data were obtained at pH 6.8−12.4 from the initial rates of O_2 evolution using linear portions of the entire kinetic curves. Each initial rate reported is a mean value of three determinations.

Results

Peroxidase-Like Activity of Iron(III)−TAML Activators. To a certain extent, Fe^{III}−TAML activators **1** are structurally reminiscent of porphyrinatoiron(III) complexes, which are known to form dimers in aqueous solution.[44] The dimerization of heme, which noticeably affects the catalytic activity in reactions with hydrogen peroxide,[45] can be followed by UV/vis spectroscopy—the observed extinction coefficients depend strongly upon the concentrations of heme. Therefore, the spectral properties of **1c** have been investigated over the wide concentration range of 1.84×10^{-6}−2.30×10^{-3} M at pH 7.0. In contrast with iron(III) porphyrins, Fe^{III}−TAML activators show no evidence for aggregation as suggested by the constancy of the extinction coefficient of **1c** over the entire concentration range (Figure 1S). This was important to establish, because our initial kinetic studies of the **1**-catalyzed oxidation/bleaching of Pinacyanol chloride (Chart 2) in the presence of **1a** revealed complicated kinetics. At pH 11, in particular, the initial rate passes through a maximum with increasing the dye concentration.

Therefore, Pinacyanol chloride is not a useful electron donor for mechanistic studies of the Fe^{III}−TAML-catalyzed oxidations such that alternative reducing agents were sought as follows. A key challenge for parametrizing the peroxidase behavior was to find reaction conditions where the kinetics of the interactions of Fe^{III}−TAML catalysts with H_2O_2 would be rate-determining and where, preferably, the rate of formation of the Fe^{III}−TAML reactive intermediates could be obtained. It was essential to find a fast reacting substrate where the oxidation process could also be followed in a straightforward experimental manner over all pHs and temperatures of interest such that the peroxidase-like oxidation of the substrate would occur in a fast step after the reactions to form the reactive intermediate(s). It has recently

Chart 2. Water-Soluble Organic and Inorganic Ruthena(II)cyclic Dyes (**2**) Used in This Study

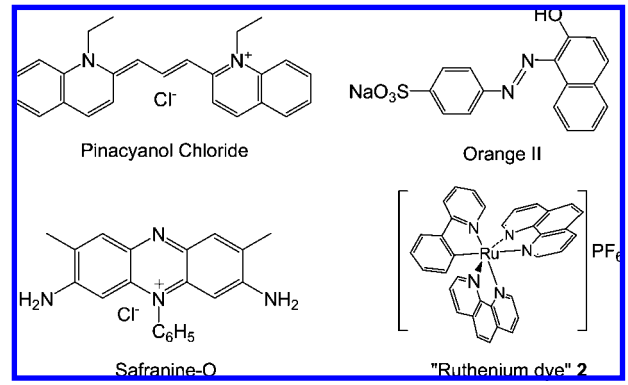

been demonstrated that cyclometalated Ru^{II} complexes of the type $[Ru(C\sim N)(LL)_2]PF_6$ (**2**; C∼*N* = cyclometalated 2-phenylpyridine or 4-tolylpyridine, LL = bpy or phen) are very reactive electron donors toward peroxidases from different sources—the Ru^{III}/Ru^{II} redox potentials are around 200 mV (versus SCE).[39,46] The rate constants for oxidation to their Ru^{III} forms measured under the steady-state conditions are higher than 10^7 M^{-1} s^{-1}. Complexes such as **2** are inert to ligand substitution and their redox potentials are pH invariant in the range 6−11.5. Therefore, the **2** substrates were selected for kinetic studies of the peroxidase-like activity of **1**. A clean conversion of Ru^{II} into Ru^{III} is accompanied by an UV/vis absorbance decrease around 500 nm and an isosbestic point holds at 400 nm (Figure 1). Exactly 1 mol of H_2O_2 oxidizes 2 moles of Ru^{II} in accord with the stoichiometry of equation 1.

$$[Ru^{II}] + 1/2\ H_2O_2 + H^+ \xrightarrow{Fe^{III}-TAML} [Ru^{III}] + H_2O \qquad (1)$$

The stoichiometry has been verified as described elsewhere[47] by consecutive additions of aliquots of H_2O_2 to the buffered solution containing **2** and the Fe^{III}−TAML catalyst. Importantly, the relation [**2**] > [H_2O_2] can be set to reduce intrusion of the catalase-like activity. The concentration of oxidized Ru^{II} is plotted against the added concentration of H_2O_2 to give a straight line with the slope of 2.0 ($r^2 = 0.99$) (Inset to Figure 1). Both oxidation equivalents of H_2O_2 are thus delivered by Fe^{III}−TAMLs to the ruthenium complex and competition from catalase activity has been eliminated. By using ferrocene as an electron donor and monitoring its oxidation into the ferricenium cation at 618 nm,[47,48] we have similarly confirmed the total selectivity of the Fe^{III}−TAML/H_2O_2 catalytic system that can be achieved for certain peroxidase-like transformations.

The kinetics of reaction 1 using different TAML activators **1** has been investigated over a wide pH range by following decreases in absorbance at 480 nm attributable to the oxidation of Ru^{II} to Ru^{III}. The resulting enzyme-like kinetic traces exhibit no induction periods. They do not display curvature until degrees of conversion around 85% are reached suggesting zero order dependence in the concentration of **2**. Absorbance changes in the absence of **1** were found to be negligible under these conditions. The steady-state rates have been measured at

(44) Brown, S. B.; Dean, T. C.; Jones, P. *Biochem. J.* **1970**, *117*, 733–739.
(45) Brown, S. B.; Dean, T. C.; Jones, P. *Biochem. J.* **1970**, *117*, 741–744.
(46) Alpeeva, I. S.; Soukharev, V. S.; Alexandrova, L.; Shilova, N. V.; Bovin, N. V.; Csoregi, E.; Ryabov, A. D.; Sakharov, I. Y. *J. Biol. Inorg. Chem.* **2003**, *8*, 683–688.
(47) Goral, V. N.; Nelen, M. I.; Ryabov, A. D. *Anal. Lett.* **1995**, *28*, 2139–2148.
(48) Ryabov, A. D.; Goral, V. N. *J. Biol. Inorg. Chem.* **1997**, *2*, 182–190.

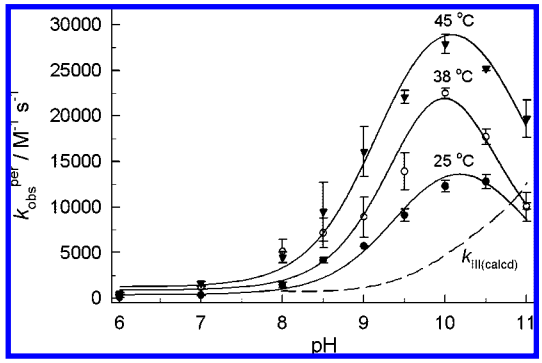

Figure 2. pH profiles of the rate constants k_{obs}^{per} for the oxidation of **2** by H_2O_2 catalyzed by **1c** at different temperatures. Conditions: [**1c**] 1.28 × 10^{-7} M, [**2**] 5.81 × 10^{-5} M, [H_2O_2] 3.3 × 10^{-4} M, 0.01 M phosphate buffer. Dashed line shows the calculated dependence of k_{III} versus pH, see text for details.

different concentrations of **1c** (3.20 × 10^{-8}−4.80 × 10^{-7} M), H_2O_2 (8.25 × 10^{-5}−1.11 × 10^{-3} M), and **2** (2.58 × 10^{-5}−1.96 × 10^{-4} M). As anticipated, the rates are directly proportional to the concentrations of all Fe^{III}−TAML activators studied implying first order dependences on **1**. First order dependence has also been observed in the H_2O_2 concentration. The steady-state rate is independent of the **2** concentration. The zero order dependency in the Ru^{II} complex and the first order dependence in H_2O_2 both hold over the *entire pH range* investigated (6−11.5). Thus, the experimental rate law given by eq 2 suggests that the rate limiting step involves the interaction between **1** and H_2O_2, which is then followed by fast oxidation of the substrates.

$$\text{rate} = k_{obs}^{per}[\mathbf{1}][H_2O_2] \qquad (2)$$

Equation 2 emphasizes advantages of the Ru^{II} complex, **2**, as an electron donor in studies of **1**-catalyzed oxidations by H_2O_2. The rate law of eq 2 holds at all pHs, despite the fact that k_{obs}^{per} is strongly pH-dependent (see below).

Free radical oxidation chemistry[23] appears not to be involved in these Fe^{III}−TAML catalyzed oxidations to any detectable degree. The efficient hydroxyl radical scavenger, mannitol,[49,50] when added over the concentration range (0.5−2.0) × 10^{-3} M has no effect on the rate of reaction 1 catalyzed by **1c** (3.6 × 10^{-7} M) at pH 9.0. We conclude that this peroxide oxidation catalyzed by **1** does not proceed extensively via the hydroxyl free radical serving as the reactive intermediate. In addition, ample evidence suggests that the rate-limiting step is not trivial substitution of axial water by H_2O_2 in the coordination sphere of **1**. The lower limit of the pseudo-first order rate constant for the water exchange k_{ex} for **1** is 2 × 10^5 s^{-1} at pH 9.2 and 25 °C, where $k_{ex} = k_{intrinsic}[H_2O]$.[42] Because H_2O and H_2O_2 are similar as ligands, one can suggest that they would exhibit comparable rate constants for ligand exchange. Thus, the rate constant k_{obs}^{per} at the highest H_2O_2 concentration used (~10^{-3} M) would have to be around 2 × 10^8 M^{-1} s^{-1} if ligand exchange is rate determining and this value is 4 orders of magnitude higher than those reported in Figure 2.

The dependencies of k_{obs}^{per} on pH for **1c** at 25−45 °C are shown in Figure 2. The rate constant increases dramatically at pH > 9 reaching a maximum around 10.0 and declines at higher pHs.

Scheme 1. Stoichiometric Mechanism of Activation of H_2O_2 by Fe^{III}−TAMLs Proposed to Account for the pH Dependence of the Rate Constant k_I

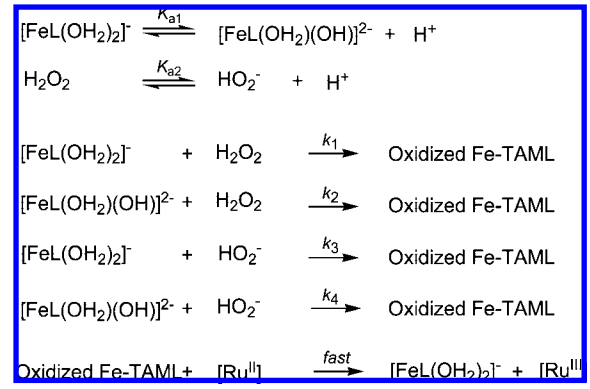

These dependencies are analyzed in what follows using a conventional approach as shown in Scheme 1.[51,52] The pH profiles in Figure 2 are rationalized quantitatively using the known pK_a's of the catalysts[53] and H_2O_2.[54] The iron(III)−TAML activators reported in this study are almost certainly all six-coordinate in water with two axial aqua ligands with the first pK_{a1}'s lying in the range 9−10.[53] The diaqua and aqua/hydroxo Fe^{III} complexes are likely reactive species that interact pairwise with either H_2O_2 or its conjugate base (pK_{a2} ≈ 11.2−11.6[54]) with the rate constants k_1−k_4 to give an oxidized Fe−TAML, the nature of which is the subject of ongoing study. We have recently characterized the first authentic iron(V)oxo complex, which was produced from **1a** and *m*-chloroperoxybenzoic acid at low temperatures (−60 °C) in a nonaqueous solvent.[55] In water (pH > 12), the observed product from **1a** and H_2O_2 is the iron(IV)oxo complex,[56] which has similar features with $[(H_2O)_5Fe^{IV}{=}O]^{2+}$.[57] It is possible, even likely, that these five-coordinate species (or relatives with a sixth aqua or hydroxo ligand) play a role in the chemistry that we are describing here. The oxidized Fe−TAML reacts with **2** very fast (Scheme 1) and therefore the reactions between the iron(III)−TAMLs and hydrogen peroxide are formally irreversible.[52] Scheme 1 leads to the rate expression 3 with kinetically indistinguishable k_2 and k_3 pathways. The experimental data have been fitted to eq 3 neglecting either k_2 or k_3 pathways.

$$k_{obs}^{per} = \frac{k_1[H^+]^2 + (k_2K_{a1} + k_3K_{a2})[H^+] + k_4K_{a1}K_{a2}}{[H^+]^2 + (K_{a1} + K_{a2})[H^+] + K_{a1}K_{a2}} \qquad (3)$$

This allowed calculation of the rate constants k_2 or k_3, respectively, as well as k_1 and k_4. The best fit values for the

(49) Halliwell, B.; Gutteridge, J. M. *Arch. Biochem. Biophys.* **1986**, *246*, 501–514.
(50) Halliwell, B.; Gutteridge, J. M. *Methods Enzymol.* **1990**, *186*, 1–85.
(51) Bender, M. L.; Bergeron, R. J.; Komiyama, M. *The Bioorganic Chemistry of Enzymatic Catalysis*; John Wiley & Sons: New York, 1984.
(52) Espenson, J. H. *Chemical Kinetics and Reaction Mechanisms*, 2nd ed.; McGraw-Hill, Inc.: New York, 1995.
(53) Ghosh, A.; Ryabov, A. D.; Mayer, S. M.; Horner, D. C.; Prasuhn, D. E., Jr.; Sen Gupta, S.; Vuocolo, L.; Culver, C.; Hendrich, M. P.; Rickard, C. E. F.; Norman, R. E.; Horwitz, C. P.; Collins, T. J. *J. Am. Chem. Soc.* **2003**, *125*, 12378–12378.
(54) Jones, C. W. *Applications of hydrogen peroxide and derivatives*; The Royal Society of Chemistry: Cambridge, 1999.
(55) Tiago de Oliveira, F.; Chanda, A.; Banerjee, D.; Shan, X.; Mondal, S.; Que, L., Jr.; Bominaar, E. L.; Muenck, E.; Collins, T. J. *Science* **2007**, *315*, 835–838.
(56) Chanda, A.; Shan, X.; Chakrabarti, M.; Ellis, W.; Popescu, D.; Tiago de Oliveria, F.; Wang, D.; Que, L., Jr.; Collins, T. J.; Münck, E.; Bominaar, E. L. *Inorg. Chem.* **2008**, *47*, 3669–3678.
(57) Pestovsky, O.; Stoian, S.; Bominaar, E. L.; Shan, X.; Munck, E.; Que, L., Jr.; Bakac, A. *Angew. Chem., Int. Ed.* **2005**, *44*, 6871–6874.

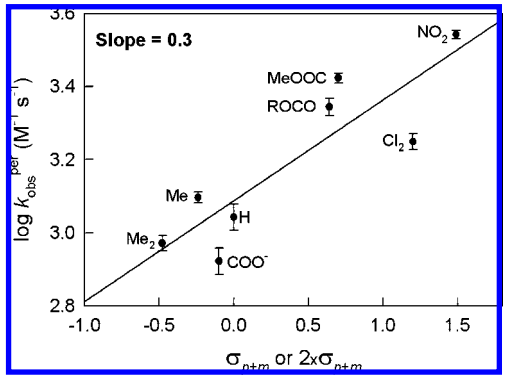

Figure 3. Hammett plot for the oxidation of **2** by H_2O_2 catalyzed by head-substituted iron(III) activators at pH 9 and 25 °C.

rate and equilibrium constants (Table 1) have been used for the emulation of the solid lines in Figure 2. The enthalpies and entropies of activation for each pathway ($\Delta H^{\ddagger}$ and $\Delta S^{\ddagger}$, Table 1) have been obtained by plotting ln(k/T) versus T^{-1}.[52] Errors in k as weights were used in these calculations.

The numerical values of the rate constants in Table 1 suggest a possible discrimination between the kinetically indistinguishable pathways k_2 and k_3. If one assumes that $k_2 = 0$, then $k_3 \approx 10^6$ M^{-1} s^{-1}. This is perhaps too high for nonenzymatic activation of H_2O_2 (see Discussion section). A more realistic rate constant $k_2 = 1.8 \times 10^4$ M^{-1} s^{-1} at 25 °C (if $k_3 = 0$) is still very high for a low molecular weight synthetic activator of H_2O_2. The rate constants k_1 and k_4 are by a factor of ca. 100 and 10 lower compared to k_2, respectively, and this accounts for the sharp maxima in Figure 2. Since the different **1** catalysts contain TAMLs of significantly dissimilar donor capacities, a trend in variation of the intrinsic rate constants k_1−k_4 is anticipated because the interaction between **1** and hydrogen peroxide is a redox reaction combining both binding of H_2O_2 to the Fe^{III}−TAMLs and decomposition of the peroxide to an oxo ligand and water. The deprotonated species $[FeL(OH)(H_2O)]^{2-}$ is more electron rich than $[FeL(H_2O)_2]^{-}$ and therefore it is reasonable to conclude that H_2O_2 would oxidize the former much faster than the latter ($k_2 \gg k_1$). Deprotonated hydrogen peroxide HO_2^- is more electron rich than H_2O_2 and therefore it may react slower with $[FeL(OH)(H_2O)]^{2-}$ ($k_2 > k_4$) because a Coulombic factor may also affect this step. Of course, these arguments are a posteriori rationalizations of the observed pH dependencies.

The values of log k_{obs}^{per} do not correlate as might be expected with the reduction potentials of **1**, which have been measured in acetonitrile by cyclic voltammetry (see Supporting Information). Interestingly, the Hammett plot in Figure 3 reveals that **1** activators that are less electron-rich react slightly faster with H_2O_2 at pH 9—the parameter ρ equals +0.3. This appears to be perplexing at first glance because while the substituent effect is minor, it suggests that the "head" ring-substituents are controlling the relative rates of a process that is favored by a more Lewis acidic metal center. The rates of both the ligand exchange and oxidation reactions ought to be favored by a greater electron density at the metal. However, the oxidation process that results in splitting of the O−O bond of H_2O_2 after its coordination needs also to be considered, as this presumably also requires proton transfers from the coordinated hydrogen peroxide. Scheme 2 presents a more detailed analysis than the minimalist version used for the kinetic treatment (Scheme 1). The details in Scheme 2 depict suggestions for the underlying sequence of additional events between the starting Fe^{III}−TAML and the final iron(V)oxo complex, suggested here in water and observed in nonaqueous solvents.[55] The peroxide ligand deprotonation associated with the equilibria K_1^a and K_2^a should be enhanced by an increase in the Lewis acidity of the iron. Such a deprotonation would result in a rehybridization of the coordinated O-atom and an increase in bonding with iron favorable for a liberation of water or hydroxide by heterolytic cleavage of the O−O bond. An alternative process whereby the proton on the coordinated O-atom tautomerizes by moving to the uncoordinated O-atom to facilitate release of water is also possible, but this process seems less likely at pH 9 given that the so-formed [Fe−O−OH_2] species could be expected to be quite acidic.

It is not known in water if the proposed **3** complex, observed in nonaqueous solvents, is formed. An alternative formulation would have the hydroxo ligand still coordinated to iron and this hypothetical species **4** could also be deprotonated to give a *trans*-dioxo species. In fact, our mechanistic theory for the pH dependent rate of interaction Fe^{III}−TAML complexes with H_2O_2 is consistent with there being more than one iron(V) reactive intermediate. When Fe^{III}−TAML complexes are reacted with excess peroxide in water and in the absence of substrates, only Fe^{IV} complexes can be observed, produced possibly by the rapid conproportionation of the Fe^{III} and Fe^{V} species, or perhaps even from **3** or **4** via catalase type reduction.

Catalase Activity of Iron(III)−TAML Activators. In the absence of electron donors, complexes **1** display a catalase-like activity (eq 4). Dioxygen evolution can be visually observed at $[H_2O_2] > 0.01$ M. This catalytic feature has been studied kinetically by monitoring the initial rates of O_2 formation with a Clark electrode.

$$H_2O_2 \xrightarrow{Fe^{III}-TAML} H_2O + 1/2\ O_2 \qquad (4)$$

The reaction stoichiometry is given in eq 4 (see Supporting Information). A linear dependence was observed when the concentration of added H_2O_2 was plotted against the concentration of O_2 formed in the presence of **1a** at pH 10.3 and 25 °C (Figure 2S, Supporting Information). The slope equals 0.45 ± 0.01 ($r^2 = 0.98$), close to 0.5 in accordance with eq 4. Reaction 4 follows first-order kinetics in **1** ((0.6 to 9) × 10^{-6} M for **1a**−**d**) and H_2O_2 (2.3×10^{-4} to 0.157 M) in the absence of an electron donor. Thus, the rate expression 5 holds for the catalase-like activity, which is identical to eq 2 for the peroxidase-like activity.

$$\text{rate} = k_{obs}^{cat}[\mathbf{1}][H_2O_2] \qquad (5)$$

The rate constants k_{obs}^{cat} are again pH-dependent (Figure 4) and the pH profiles for reactions 2 (Figure 2) and 4 (Figure 4), both catalyzed by **1c**, are similar. Equation 3 has therefore also been applied for fitting the data in Figure 4. The best fit rate and equilibrium constants are summarized in Table 2. For the reasons discussed above, the rate constants k_3 are not included in Table 2. The rate constants in Tables 1 and 2 indicate that the catalase-like (also referred to as "catalatic") rate constants are somewhat lower than the peroxidase-like (also referred to as "peroxidatic") rate constants. The data for reactions 2 and 4 have been obtained in 0.01 and 0.10 M phosphate, respectively, because a higher buffer concentration improves the reproducibility of the Clark electrode data. Through careful checking, it has been found that the rate of reaction 4 is virtually independent of the buffer concentration. To derive the activation parameters,

Scheme 2. More Extensive Picture of the Mechanistic Events Proposed to Play a Role in the k_1 and k_2 Pathways of Formation of an Iron(V)oxo Intermediate

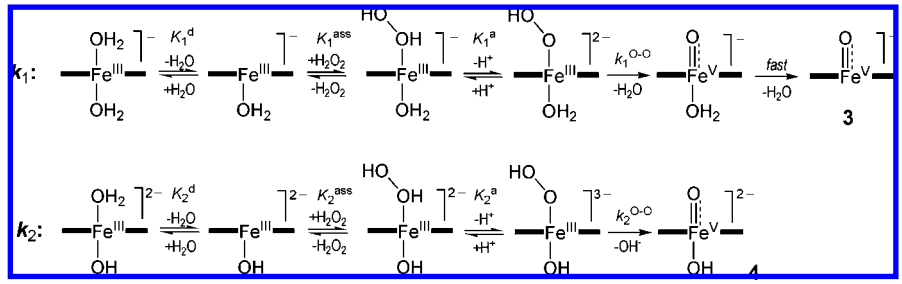

the temperature dependence of k_{obs}^{cat} has been investigated from 25−45 °C at pH 10.1. At this pH, the k_2 pathway dominates—its contribution into the overall rate is more than 99%. Therefore, the effective enthalpy of activation obtained from the temperature dependence of k_{obs}^{cat} is associated with $\Delta H^{\ddagger}$ for the k_2 pathway. The corresponding $\Delta S^{\ddagger}$ has been calculated using k_2 from Table 2; the calculated $\Delta H_2^{\ddagger}$ and $\Delta S_2^{\ddagger}$ are shown in a footnote to Table 2.

Scheme 3. Stoichiometric Mechanism of Catalysis by Fe^{III}−TAMLs Proposed to Rationalize the Peroxidase- and Catalase-Like Activities of **1**

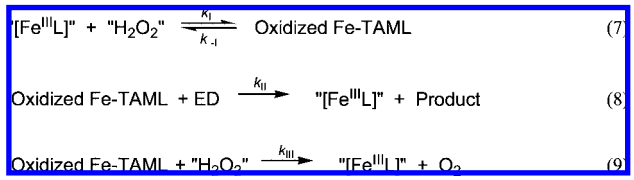

Evidence for a Common Intermediate. The similar rate laws (eqs 2 and 5), pH profiles (Figures 2 and 4), and the values of the observed second order rate constants (k_{obs}^{per} and k_{obs}^{cat}) suggest a common reaction intermediate in reactions 1 and 4 (Oxidized Fe−TAML in Scheme 1). A plausible stoichiometric mechanism accounting for both catalytic features of Fe^{III}−TAMLs is presented in Scheme 3 with the term "Oxidized Fe−TAML" being used to denote our uncertainty over the exact nature of the reactive species associated with the k_{II} and k_{III} pathways. Taking all three steps into consideration, the rate of the peroxidase-like activity of **1** is given by eq 10,

$$rate = \frac{k_I k_{II}[\text{Fe−TAML}][H_2O_2][ED]}{k_{-I} + [H_2O_2](k_I + k_{III}) + k_{II}[ED]} \quad (10)$$

where ED is any appropriate electron donor, an organic dye or ruthenium dye **2**. The catalase-like activity is described by eq 11.

$$rate = \frac{k_I k_{III}[\text{Fe−TAML}][H_2O_2]^2}{k_{-I} + [H_2O_2](k_I + k_{III}) + k_{II}[ED]} \quad (11)$$

Equations 10 and 11 were derived applying the steady state approximation to the oxidized Fe−TAML and using the mass balance equation [Fe−TAML] = **1** + [oxidized Fe−TAML] ([Fe−TAML] is the *total* concentration of all iron species, which is significantly lower than the concentrations of H_2O_2 and ED). The oxidation of ruthenium dye **2** is a zero order reaction in **2**. This implies that $k_{II}[ED] \gg \{k_{-I} + [H_2O_2](k_I + k_{III})\}$. Equation 10 becomes very simple, that is,

$$\frac{\text{rate}}{[\text{Fe−TAML}][H_2O_2]} = k_{obs}^{per} = k_I \quad (12)$$

First order dependence in hydrogen peroxide for the catalase-like activity holds when $[H_2O_2](k_I + k_{III}) \gg k_{-I} + k_{II}[ED]$. Then, in the absence of added ED, eq 11 becomes

$$\frac{\text{rate}}{[\text{Fe−TAML}][H_2O_2]} = k_{obs}^{cat} = \frac{k_I k_{III}}{k_I + k_{III}} \quad (13)$$

Thus, both the peroxidase-like and catalase-like reactions have similar rate laws and the effective second order rate constant k_{obs}^{cat} should practically equal k_{obs}^{per} (when $k_{III} > k_I$) or it should be lower than k_{obs}^{per} when otherwise, provided k_{obs}^{per} is zero order in ED. The conditional rate constants k_I and k_{III} are pH dependent. The data in Figures 2 and 4 allow us to estimate the dependence of the rate constant k_{III} on pH using eqs 12 and 13. Thus, the calculated plot of k_{III} versus pH in the range 8−11, where the accuracies in measuring k_{obs}^{per} and k_{obs}^{cat} are the highest, is shown as a dashed line in Figure 2. Under these conditions, k_{III} is somewhat lower than k_I. This is consistent with the fact that registration of the product/s of interaction between complexes **1** and H_2O_2 by spectral techniques is feasible even in the presence of an excess of the oxidizing agent.[56] The shape of

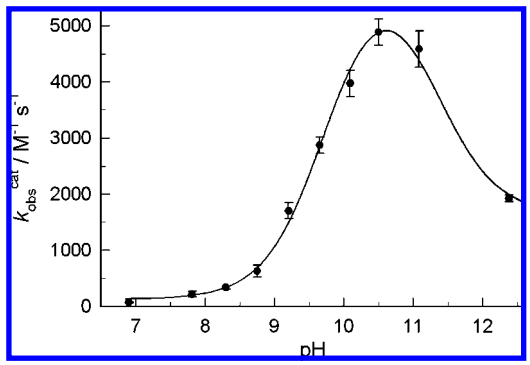

Figure 4. pH profiles of the second order rate constants k_{obs}^{cat} for the disproportionation of H_2O_2 catalyzed by **1c** at 25 °C in 0.1 M phosphate.

Table 2. Rate (in M^{-1} s^{-1}) and Equilibrium Constants and Activation Parameters for Iron(III)−TAML Catalyzed Disproportionation of Hydrogen Peroxide (eq 4) at 25 °C and 0.1 M Phosphate

Fe^{III}−TAML	$10^{-2} \times k_1$	$10^{-4} \times k_2$	$10^{-3} \times k_4$	pK_{a1}	pK_{a2}
1a	1.4 ± 1.2	0.51 ± 0.03[a]	[b]	11.0 ± 0.2	12.1 ± 0.4
1b	4.3 ± 1.8	0.90 ± 0.06	0.87 ± 0.6	11.0 ± 0.2	12.15 ± 0.35
1c	1.3 ± 0.7	0.64 ± 0.04[c]	1.6 ± 0.2	9.75 ± 0.11	11.3 ± 0.3
1d	6 ± 3	1.68 ± 0.08[d]	3.2 ± 0.2	10.5 ± 0.2	11.6 ± 0.2

[a] $\Delta H^{\ddagger}$ 23 ± 3 kJ mol^{-1}; $\Delta S^{\ddagger}$ −95 ± 20 J mol^{-1} K^{-1}. [b] Could not be reliably estimated. [c] $\Delta H^{\ddagger}$ 15 ± 1 kJ mol^{-1}; $\Delta S^{\ddagger}$ −120 ± 10 J mol^{-1} K^{-1}. [d] $\Delta H^{\ddagger}$ 8 ± 3 kJ mol^{-1}; $\Delta S^{\ddagger}$ −140 ± 60 J mol^{-1} K^{-1}.

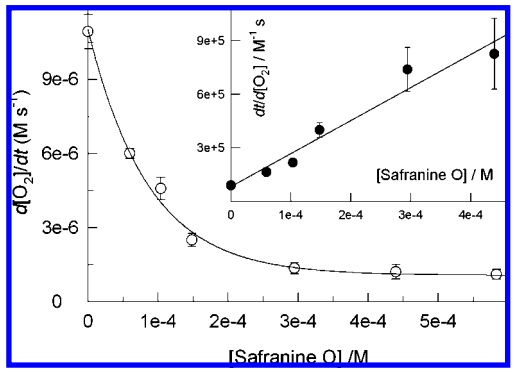

Figure 5. Retardation of the catalase activity of activator **1d** by the dye Safranine O as an electron donor. Conditions: $[H_2O_2]$ 2.65×10^{-3} M, [**1d**] 1.18×10^{-6} M, pH 10, 25 °C. (Inset) Rate of O_2 evolution is inversely proportional to [Safranine O].

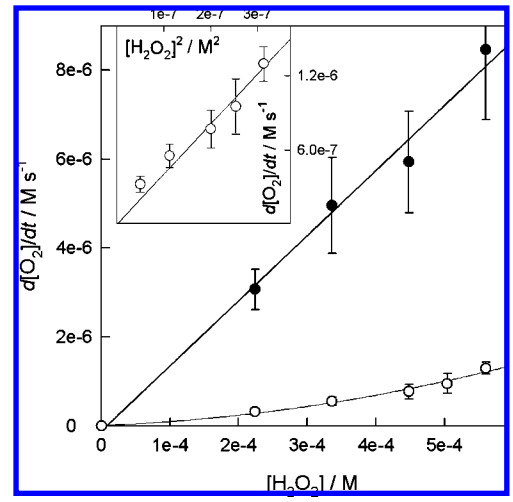

Figure 6. Kinetics of the Fe^{III}−TAML **1c**-catalyzed O_2 evolution in the absence (*a*) and in the presence of Safranine O (6×10^{-4} M) (*b*). Conditons: [**1c**] 8.8×10^{-6} M, pH 11, 25 °C. (Inset) Emphasis on the second order in $[H_2O_2]$ induced by Safranine O.

the pH profile for k_{III} in Figure 2 can be qualitatively understood as follows. Hydrogen peroxide becomes a better reducing agent upon deprotonation and therefore the rate constant k_{III} starts to rise at pH > 10.[58]

The postulated identities of the oxidized Fe−TAMLs in the peroxidase-like and catalase-like reactions sets up the question of whether 100% oxidative efficacy (quantitative peroxidase-like activity) can be achieved for **1**. If reactions 1 and 4 involve the same intermediate, ED and H_2O_2 should compete for it and the peroxide could be wasted. Once formed (k_I), oxidized Fe−TAML reacts either with an electron donor (ED) (peroxidase-like activity: k_{II}) or a second H_2O_2 molecule to produce O_2 (catalase-like activity: k_{III}). At a given pH, 100% efficacy is observed if $k_{II}[ED] \gg k_{III}[H_2O_2]$, i.e. when the oxidized Fe−TAML reacts faster with ED than with H_2O_2. Previously, we have measured k_{II} for some dyes[32,59] but the rate constants k_{III} for step 9 cannot be measured directly under steady state conditions (unless $k_{III} \ll k_I$). The ratio k_{II}/k_{III} can be estimated by measuring the rate of O_2 evolution in the presence of variable ED concentrations using eq 11. The rate of O_2 formation should be retarded hyperbolically with increasing [ED] and this has been confirmed by using the dyes Safranine O and Orange II as electron donors.

The catalase-like activity of Fe^{III}−TAML activator **1d** does decrease in the presence of Safranine O (Figure 5). The inset to Figure 5 shows that the plot of the inverse rate versus [Safranine O] is a straight line consistent with eq 14.

$$\frac{[\text{Fe}-\text{TAML}][H_2O_2]}{\text{rate}} = \frac{k_I + [H_2O_2](k_I + k_{III})}{k_I k_{III}[H_2O_2]} + \frac{k_{II}[ED]}{k_I k_{III}[H_2O_2]} \approx \frac{k_I + k_{III}}{k_I k_{III}} + \frac{k_{II}[ED]}{k_I k_{III}[H_2O_2]} \quad (14)$$

The intercept and slope equal $(k_I + k_{III})/k_I k_{III}$ and $k_{II}/k_I k_{III}[H_2O_2]$, respectively. An estimate for the ratio k_{II}/k_{III} is derived from the slope using the known value of k_I (e.g., 4.4×10^3 M^{-1} s^{-1} for **1d**). The k_{II}/k_{III} ratio equals 52 for **1d** and indicates that the oxidized Fe−TAML is significantly more reactive to the ED, Safranine O, than to H_2O_2. This extremely important feature of the Fe^{III}−TAML activators eliminates unproductive decomposition of H_2O_2 in the oxidation of Safranine O and, similarly, provides a rationale for the 100% efficacy with respect to H_2O_2 in reactions with complex **2** and with ferrocene. Similarly, H_2O_2 is not wasted at neutral pH for processes such as the oxidation of dibenzothiophenes, which do not occur readily at pH >10.[60]

Observing the Invisible: Masked Second Order Kinetics in H_2O_2. The case for involvement of a similar reactive intermediate in both reactions 1 and 4 can further be strengthened. The rate law 11 shows that O_2 formation is always first order in H_2O_2 at [ED] = 0 and negligible k_{-1}. When ED is in large excess, then $(k_I + k_{III})[H_2O_2] \ll k_{II}[ED]$ and eq 11 becomes eq 15, predicting a second order dependence in H_2O_2.

$$\text{rate} = \frac{k_I k_{III}[\text{Fe}-\text{TAML}][H_2O_2]^2}{k_{II}[ED]} \quad (15)$$

The "large excess" situation is actually a hypothetical case because the resulting large denominator in eq 11 would result in no O_2 evolution being observed. However, an intermediate case is experimentally feasible where ED concentrations are both low enough so as not to totally suppress O_2 evolution, but high enough so that eq 11 is still operative. If such conditions could be found, we hypothesized that O_2 evolution would be found to be second order in $[H_2O_2]$. While finding clear evidence for second order kinetics required that a considerable concentration range of H_2O_2 should be covered, we also realized that the relation $(k_I + k_{III})[H_2O_2] \ll k_{II}[ED]$ would at some point become invalid such that the reaction order should descend from 2 becoming exactly 1 in the limiting case when $(k_I + k_{III})[H_2O_2] > k_{II}[ED]$. Thus, we searched the H_2O_2 concentration space for these different $[H_2O_2]$-dependent behaviors.

The system H_2O_2−Safranine O−**1d** allow experimental observation of all three cases mentioned above (Figure 6). When no Safranine O is present, reaction 4 is strictly first order in H_2O_2. At 6×10^{-4} M Safranine O, the rate is nonlinear function of the H_2O_2 concentration. The inset to Figure 6 shows that the

(58) The reduction potential for the half-reaction, $O_2 + 2\ H_2O + 2e \rightarrow H_2O_2 + 2\ OH^-$, equals−0.146 V: Lide, D. R., Ed. *CRC Handbook of Chemistry and Physics*, 87th ed.; CRC Taylor & Francis: New York, 2006−2007.

(59) Chanda, A.; Ryabov, A. D.; Mondal, S.; Alexandrova, L.; Ghosh, A.; Hangun-Balkir, Y.; Horwitz, C. P.; Collins, T. J. *Chem.−Eur. J.* **2006**, *12*, 9336–9345.

(60) Hangun, Y.; Alexandrova, L.; Khetan, S.; Horwitz, C.; Cugini, A.; Link, D. D.; Howard, B.; Collins, T. J. *Prepr. Am. Chem. Soc., Div. Petr. Chem.* **2002**, *47*, 42–44.

Scheme 4. Accepted Mechanism of Catalysis by Peroxidase Enzymes

$$E(Fe^{III}, \text{porphyrin}) + H_2O_2 \rightarrow \underset{\textbf{Compound I}}{E(Fe^{IV}, \text{porphyrin}^{+\bullet})} + H_2O \quad (k_{12}) \quad (12)$$

$$E(Fe^{IV}, \text{porphyrin}^{+\bullet}) + ED \rightarrow \underset{\textbf{Compound II}}{E(Fe^{IV}, \text{porphyrin})} + ED^{+\bullet} \quad (k_{13}) \quad (13)$$

$$E(Fe^{IV}, \text{porphyrin}) + ED \rightarrow E(Fe^{III}, \text{porphyrin}) + ED^{+\bullet} \quad (k_{14}) \quad (14)$$

$$ED^{+\bullet} \rightarrow \rightarrow \rightarrow \text{various products} \quad (15)$$

oxygen evolution follows the second-order kinetics in H_2O_2 at concentrations below 3×10^{-3} M. As the $[H_2O_2]$ increases, intermediate orders in H_2O_2 develop and then prevail. These results provide strong evidence for the involvement of a second H_2O_2 molecule in the dioxygen evolution in step 9. More intimate mechanistic details of this process are under examination.

Discussion

The studies described above demonstrate that Fe^{III}−TAML activators are functional models of catalase−peroxidase enzymes. They display both catalase-like and peroxidase-like activities, both subject to control by the addition of suitable electron donors. The catalase-like activity is negligible in the presence of the electron donors and therefore both oxidizing equivalents of H_2O_2 are economically used in the Fe^{III}−TAML catalyzed oxidations for the presented substrates. Of course, as the ED becomes progressively more difficult to oxidize, it is anticipated that the efficiency will begin to fall in favor of the catalase-like reaction channel.

Peroxidase-Like Activity of Fe^{III}−TAML Activators. Fe^{III}−TAML activator catalysis is distinct from the diverse family of peroxidase enzymes in terms of the usual rate determining step.[2,61] The enzymes usually activate H_2O_2 to form Compound I faster than they oxidize EDs via the intermediate formation of Compound II (peroxidase-like activity, Scheme 4) or react with hydrogen peroxide to form dioxygen (catalase-like activity). For the purposes of comparison, numerous enzymatic k_{12} values have been obtained, which can be contrasted with the k_I values for **1**. Since the rate-determining step for the enzymes is often not k_{12}, these comparisons give the reader a worst case estimate of the **1** performances relative to the enzymes.

For example, for horseradish peroxidase isoenzyme C the relationships among the rate constants are $k_{12} > k_{13} \gg k_{14}$.[2,61] In contrast, for the **1** activators k_I that corresponds to k_{12} in Scheme 4 is often the rate determining for EDs such as organic dyes,[32,59] as is typical of other low molecular weight catalysts.[62−64] Nevertheless, the controlling rate constants for the reaction between H_2O_2 and the **1** activators are very high and in fact are comparable to those of the slower peroxidase enzymes even if the precise rate determining steps are different. Rate constants for the activation of H_2O_2 (k_{12}) by catalases, peroxidases, catalase−peroxidases to form Compound I are summarized in Table 3—several comparative data for low molecular weight transition metal complexes are also included. Importantly, rate constants that are associated with clear-cut peroxidase-like or catalase-like activities are listed. Data related to Fenton processes[23] (trivial oxidation of transition metal complexes by H_2O_2) are omitted from consideration. The reactivity of **1** is 4 orders of magnitude higher than that of hemin (Table 3, entry 15), more than 10-fold higher than that of microperoxidase-8 (entry 14) and the less stable Fe^{III}-tetraaza^{14}annulene complex (entry 16). The nonaggregating, water soluble iron(III) 5,10,15,20-tetrakis(2,6-dimethyl-3-sulfonatophenyl)porphyrin (entry 17) has comparable reactivity to Fe^{III}−TAML activators.[65] This Fe^{III} complex exists as $[LFe(H_2O)_2]^{3-}$ in water with pK_a = 7.25. Three major pathways have been identified, viz. $[LFe(H_2O)_2]^- + H_2O_2$, $[LFe(H_2O)(OH)]^{2-} + H_2O_2$, and $[LFe(H_2O)(OH)]^{2-} + HO_2^-$ (cf. with the mechanism in Scheme 1).[65]

The rate constants for the enzymatic activation of H_2O_2 are in the range 5.4×10^5−8.0×10^7 M^{-1} s^{-1} under the optimal pH at 25 °C (Table 3). The rate constant k_2 for **1c** equals 1.8×10^4 M^{-1} s^{-1} (Table 1). Thus, **1c** is only 1 order of magnitude less reactive than some of the slower reported enzymes such as lignin peroxidase *H8* (Table 3, entry 11). Note that the peroxidases consist of 290−350 amino acid residues and range in weight from 27,000 to 50,000 Da.[66] The Fe^{III}−TAML catalysts are 50−100 times lighter and considerably more synthetically tractable from the perspective of developing commercially viable peroxide activators. If the rate constants are expressed in units of L g^{-1} s^{-1}, that is, when they refer to the activity of one gram of catalyst, the rate constant for activator **1c** is 17 L g^{-1} s^{-1} which is higher than the corresponding rate constant for lignin peroxidase (13 L g^{-1} s^{-1}, Table 3, entry 11: mw 41, 000 g mol^{-1}[67]) and is only 23 times slower than horseradish peroxidase *C* (390 L g^{-1} s^{-1}, entry 4: mw 44,000 g mol^{-1}[2]). Although the most reactive ascorbate peroxidase (2900 L g^{-1} s^{-1}, entry 1: mw 27,194 g mol^{-1}[68]) still has a 170-fold advantage, the values determined clearly indicate high comparative reactivity for Fe^{III}−TAML activators. Peroxidase enzymes exhibit low enthalpies of activation $\Delta H^{\ddagger}_{12}$ for the formation of Compound I (k_{12} step), 12, 9.6, and 22 kJ mol^{-1} for horseradish,[69] turnip,[70] and lignin[71] peroxidases, respectively. Similarly low activation barriers have been found for Fe^{III}−TAML activators (Table 1). These mechanistic similarities emphasize that Fe^{III}−TAML activators are the best functioning models of the catalase−peroxidase enzymes known to date.[20]

Catalase-Like Activity of Fe^{III}−TAML Activators. The molecular masses of heme catalases are usually significantly higher as compared to peroxidases. If expressed in L g^{-1} s^{-1}, rate constants for the Fe^{III}−TAML activators when compared with catalase from beef liver, which has a molecular weight 250 000 g mol^{-1} (Table 3, entry 13),[72] look very impressive, namely, 17 L g^{-1} s^{-1} for **1c** versus 22 L g^{-1} s^{-1} for the enzyme. Nevertheless, the catalase-like activity of the Fe^{III}−TAML activators can be suppressed by the addition of electron donors—it is negligible in the presence of the substrates tested

(61) English, A. M.; Tsaprailis, G. *Adv. Inorg. Chem.* **1995**, *43*, 79–125.
(62) Ryabova, E. S.; Dikiy, A.; Hesslein, A. E.; Bjerrum, M. J.; Ciurli, S.; Nordlander, E. *J. Biol. Inorg. Chem.* **2004**, *9*, 385–395.
(63) Marques, H. M. *Inorg. Chem.* **2005**, *44*, 6146–6148.
(64) Theodoridis, A.; Maigut, J.; Puchta, R.; Kudrik, E. V.; Van Eldik, R. *Inorg. Chem.* **2008**, *47*, 2994–3013.
(65) Zipplies, M. F.; Lee, W. A.; Bruice, T. C. *J. Am. Chem. Soc.* **1986**, *108*, 4433–4445.
(66) Sae, A. S. W.; Cunningham, B. A. *Phytochemistry* **1979**, *18*, 1785–1787.
(67) Piontek, K.; Glumoff, T.; Winterhalter, K. *FEBS Lett.* **1993**, *315*, 119–124.
(68) Hill, A. P.; Modi, S.; Sutcliffe, M. J.; Turner, D. D.; Gilfoyle, D. J.; Smith, A. T.; Tam, B. M.; Lloyd, E. *Eur. J. Biochem.* **1997**, *248*, 347–354.
(69) Hewson, W. D.; Dunford, H. B. *Can. J. Chem.* **1975**, *53*, 1928–1932.
(70) Job, D.; Ricard, J.; Dunford, H B. *Can. J. Biochem* **1978**, *56*, 702–707.
(71) Andrawis, A.; Johnson, K. A.; Tien, M. *J. Biol. Chem.* **1988**, *263*, 1195–1198.
(72) Weber, K.; Sund, H. *Angew. Chem.* **1965**, *77*, 621.

Table 3. Rate Constants k_{12} for the Formation of Compound I from H_2O_2 and selected peroxidases or catalases and for **non-Fenton** peroxidase- or catalase-related activation of H_2O_2 such as k_I by the most reactive low-molecular weight iron(III) complexes in water

entry	enzyme or metal complex with catalase-like or peroxidase-like activity	pH (*T*/°C)	rate constant/M^{-1} s^{-1}	reference
1	Pea cytosolic ascorbate peroxidase	7.8 (20)	8.0×10^7	89
2	Yeast cytochrome *c* peroxidase	6.1 (25)	3.4×10^7	90
3	Yeast cytochrome *c* peroxidase	6.1 (25)	1.4×10^7	91
4	Horseradish peroxidase	4.7 (25)	1.7×10^7	92
5	Myeloperoxidase (*H. sapiens*)	7.0 (25)	2.3×10^7	93
6	Manganese peroxidase (*P. chrysosporium*)	4.5 (28)	2.0×10^6	94
7	Soybean cytosolic ascorbate peroxidase	7.0 (20)	3.3×10^7	95
8	Chloroperoxidase (*Caldariomyces fumago*)	4.7 (25)	2.4×10^6	96
9	Hog thyroid peroxidase	7.5 (20)	7.8×10^6	97
10	Turnip peroxidase P7	3.5 (25)	1.6×10^6	70
11	Lignin peroxidase H8 (*P. chrysosporium*)	3.5 (25)	5.4×10^5	71
12	Catalase (Horse erythrocyte)	6.7 (25)	3×10^7	98
13	Catalase (Beef liver)	7.0 (25)	5.6×10^6	73
14	Microperoxidase-8	5.0 (25)	680	99, 100
15	Hemin	10.0 (25)	~1	101
16	Fe^{III}-tetraaza^{14} annulene[a]	7.2 (32)	1.5×10^3	102
17	Fe^{III}−5,10,15,20-tetrakis(2,6-Me$_2$−3-sulfonatophenyl)porphyrinato	10.0 (30)	1.4×10^4[b]	65
18	[Fe^{III}(octaphenylsulfonato)porphyrazine]$^{5-}$	10.0 (25)	15	64
19	Fe^{III}−TAML activator **1c**	10.0 (25)	1.8×10^4	This work

[a]

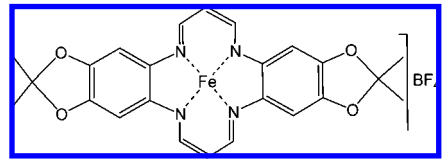

[b] 1.05×10^5 at pH 12.

Scheme 5. Speciation of Iron(IV)oxo Species in Water[56]

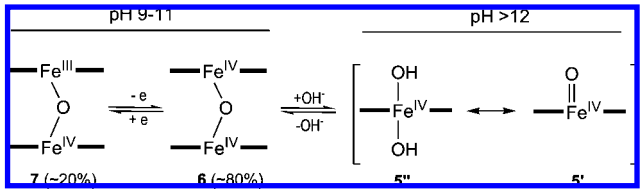

in this work. In nature, catalases display only minor peroxidase-like activity[73] because electron donors bulkier than H_2O_2 cannot access the deeply buried active sites of these massive enzymes.[6] The comparatively unprotected Fe^{III}−TAML active sites are directly exposed to electron donors such that the overall behavior is determined by the inherent relative reactivity of the substrates. The mechanism of enzymatic disproportionation of H_2O_2 involves the formation of Compound I (Step 12 in Scheme 4) followed by its reduction by the second H_2O_2 molecule, eq 16.[4,6,7]

$$E(Fe^{IV}, por^{+\bullet}) + H_2O_2 \rightarrow E(Fe^{III}, por) + O_2 + H_2O \quad (16)$$

A similar mechanism may hold for the Fe^{III}−TAML activators (cf. with steps 7 and 9 in Scheme 3). Hydrogen peroxide and EDs compete for the sterically unprotected intermediate, which is formed from **1** and H_2O_2. The reducing power of H_2O_2 is marginal. Hence, the more powerful reducing agent EDs react with oxidized Fe−TAMLs much faster, thus suppressing the catalase-like activity.

On the Nature of Oxidized Fe−TAML. Evidence has been presented[56] to show that oxidation of **1** by peroxides in water affords iron(IV) species, the distributions of which are determined by the pH (Scheme 5). These intermediates are not Fe^{III}−OOH species that have been described by different research groups.[74−87] At pH > 12 the oxoiron(IV) species **5′** dominates (>95% of total iron), but DFT studies indicate that the **5"** formulation is likely. Complex **5′** (as well as **6** and **7**) is shown as five-coordinate, though a weakly bound aqueous ligand may increase the coordination numbers of all species to six. At pH < 11, dimeric motif **6** becomes the major species. It is important to note that the spectral data used for the characterization of the oxidized Fe−TAMLs has been performed using mM solutions of **1**. The monomerization of **6** into **5** under such conditions is a bridge-splitting reaction induced by hydroxide. The kinetic data reported in this work were collected using lower

(73) Kremer, M. L. *Biochim. Biophys. Acta* **1970**, *198*, 199–209.
(74) Kim, J.; Larka, E.; Wilkinson, E. C.; Que, L., Jr. *Angew. Chem., Int. Ed. Engl.* **1995**, *34*, 2048–2051.
(75) Lubben, M.; Meetsma, A.; Wilkinson, E. C.; Feringa, B.; Que, L., Jr. *Angew. Chem., Int. Ed. Engl.* **1995**, *34*, 1512–1514.
(76) Davydov, R. M.; Smieja, J.; Dikanov, S. A.; Zang, Y.; Que, L., Jr.; Bowman, M. K. *J. Biol. Inorg. Chem.* **1999**, *4*, 292–301.
(77) Ho, R. Y. N.; Que, L., Jr.; Roelfes, G.; Feringa, B. L.; Hermant, R.; Hage, R. *J. Chem. Soc., Chem. Commun.* **1999**, 2161–2162.
(78) Simaan, A. J.; Banse, F.; Girerd, J.-J.; Wieghardt, K.; Bill, E. *Inorg. Chem.* **2001**, *40*, 6538–6540.
(79) Lehnert, N.; Ho, R. Y. N.; Que, L., Jr.; Solomon, E. I. *J. Am. Chem. Soc.* **2001**, *123*, 8271–8290.
(80) Lehnert, N.; Ho, R. Y. N.; Que, L., Jr.; Solomon, E. I. *J. Am. Chem. Soc.* **2001**, *123*, 12802–12816.
(81) Lehnert, N.; Neese, F.; Ho, R. Y. N.; Que, L., Jr.; Solomon, E. I. *J. Am. Chem. Soc.* **2002**, *124*, 10810–10822.
(82) Lehnert, N.; Fujisawa, K.; Solomon, E. I. *Inorg. Chem.* **2003**, *42*, 469–481.
(83) Chen, K.; Costas, M.; Que, J. L. *J. Chem. Soc., Dalton Trans.* **2002**, 672–679.
(84) Hazell, A.; McKenzie, C. J.; Nielsen, L. P.; Schindler, S.; Weitzer, M. *J. Chem. Soc., Dalton Trans.* **2002**, 310–317.
(85) Roelfes, G.; Vrajmasu, V.; Chen, K.; Ho, R. Y. N.; Rohde, J.-U.; Zondervan, C.; la Crois, R. M.; Schudde, E. P.; Lutz, M.; Spek, A. L.; Hage, R.; Feringa, B. L.; Muenck, E.; Que, L., Jr. *Inorg. Chem.* **2003**, *42*, 2639–2653.
(86) Neese, F.; Zaleski, J. M.; Zaleski, K. L.; Solomon, E. I. *J. Am. Chem. Soc.* **2000**, *122*, 11703–11724.
(87) Horner, O.; Jeandey, C.; Oddou, J.-L.; Bonville, P.; McKenzie, C. J.; Latour, J.-M. *Eur. J. Inorg. Chem.* **2002**, 3278–3283.

than μM concentrations of **1**. In addition to nucleophilic cleavage of the dimer, dilution provides a driving force for monomerization. It is very likely that at [**1**] $\approx 10^{-7}$ M, the dimers undergo spontaneous dissociation to form monomeric Fe^{IV} complexes. Therefore, we postulate that the monomeric iron(IV) complex may be one reactive intermediate toward **2** in the entire pH range used in this kinetic study.

An iron(V)oxo species, has been produced from **1** and organic peroxides in nonaqueous solvents.[55] While we have yet to observe this species in water, its momentary intermediacy as a reactive intermediate in water is feasible[56] though it should be very rapidly reduced by **1** as postulated for the sterically hindered anionic iron(III) porphyrins.[88] If these hypotheses hold, then the catalysis performed by Fe^{III}−TAML activators mimics remarkably well the behavior of the peroxidase enzymes.

Conclusions and Future Directions. This study has revealed the general features of hydrogen peroxide catalytic activation by iron(III)−TAML activators which display both peroxidase-like and catalase-like activity. The rate determining step of the peroxidase-like activity in the oxidation of **2** is the interaction between **1** and H_2O_2. The rate is strongly pH-dependent and the maximum activities for the different catalysts are observed at pHs around 10. The rate constants for the activation of H_2O_2 under the optimal conditions ($>10^4$ M^{-1} s^{-1}) approach the lower limit of the corresponding enzymatic peroxidase-catalyzed reactions. The comparisons made give worst case estimates for the comparable reactivity of Fe^{III}−TAML activators against peroxidase enzymes and define the former as exhibiting comparable performance to the enzymes they were designed to mimic. The activation of H_2O_2 to oxidize the one-electron transfer reducing agent, **2**, is believed to proceed via both iron(V)oxo and iron(IV)oxo (or iron(IV)dihydroxo) species. The oxidation of substrate electron donors occurs in subsequent steps. In the absence of peroxidase-like substrates, the iron(III)−TAML activators display catalase-like activity with the production of dioxygen. In addition to underscoring the basic scientific features behind the significant technological importance of Fe^{III}−TAML activators,[29,30] these results signify that the activators are prominent functional models of the catalase−peroxidase enzymes as they display both high catalase-like and peroxidase-like activities, but the latter dominates in the presence of the electron donor substrates studied other than H_2O_2 itself, thus eliminating unproductive consumption of hydrogen peroxide. This property results in high efficiency in peroxide use for the peroxidase-like reaction channel and this is an important finding for the technological significance of Fe^{III}−TAML activators.

Acknowledgment. T.J.C. thanks the Heinz Endowments, the Eden-Hall Foundation, NSF (9612990), EPA (RD83), DOE (NETL), and the Institute for Green Science for support. E.U. thanks the Howard Hughes Medical Institute for an Undergraduate Research Grant. A.G. thanks the Heinz Foundation for the award of a Theresa Heinz Environmental Scholarship.

Supporting Information Available: Spectral properties of Fe^{III}−TAML activators in aqueous phosphate buffer, the data on stoichiometry of the Fe^{III}−TAML-catalyzed disproportionation of H_2O_2, cyclic voltammograms, and the Table with reduction potentials of Fe^{III}−TAML activators in MeCN. This material is available free of charge via the Internet at http://pubs.acs.org.

JA8043689

(88) Hodges, G. R.; Lindsay Smith, J. R.; Oakes, J. *J. Chem. Soc., Perkin Trans. 2* **1998**, 617–628.
(89) Marquez, L. A.; Quitoriano, M.; Zilinskas, B. A.; Dunford, B. H. *FEBS Lett.* **1996**, *389*, 153–156.
(90) Ohlsson, P. I.; Yonetani, T.; Wold, S. *Biochem. Biophys. Acta.* **1986**, *874*, 160–166.
(91) Balny, C. A., H. S.; Yonetani, T. *FEBS Lett.* **1987**, *221*, 349–354.
(92) Dolman, D.; Newell, G. A.; Thurlow, M. D.; Dunford, H. B. *Can. J. Biochem* **1975**, *53*, 495–501.
(93) Furtmuller, P. G.; Obinger, C.; Hsuanyu, Y.; Dunford, H. B. *Eur. J. Biochem.* **2000**, *267*, 5858–5864.
(94) Kuan, I. C.; Johnson, K. A.; Tien, M. *J. Biol. Chem.* **1993**, *268*, 20064–20070.
(95) Lad, L.; M, M; Raven, E. L. *Biochemistry* **2002**, *41*, 13774–13781.
(96) Araiso, T.; Rutter, R.; Palcic, M. M.; Hager, L. P.; Dunford, H. B. *Can. J. Biochem* **1981**, *59*, 233–236.
(97) Ohtaki, S. N., H.; Nakamura, M.; Yamazaki, I. *J. Biol. Chem.* **1982**, *257*, 761–766.
(98) Chance, B. *Acta Chem. Scand.* **1947**, *1*, 236–267.
(99) Casella, L.; De Gioia, L.; Silvestri, G. F.; Monzani, E.; Redaelli, C.; Roncone, R.; Santagostini, L. *J. Inorg. Biochem.* **2000**, *79*, 31–39.
(100) Dallacosta, C.; Monzani, E.; Casella, L. *J. Biol. Inorg. Chem.* **2003**, *8*, 770–776.
(101) Uno, T.; Takeda, A.; Shimabayashi, S. *Inorg. Chem.* **1995**, *34*, 1599–1607.
(102) Paschke, J.; Kirsch, M.; Korth, H.-G.; de Groot, H.; Sustmann, R. *J. Am. Chem. Soc.* **2001**, *123*, 11099–11100.